

**COMPARISON BETWEEN PHYSICAL WEDGES  
AND VIRTUAL WEDGES IN LINAC**

**by**

**TAN ZI XIANG**

**Thesis submitted in fulfillment of the requirements for  
the degree of Master of Science (Medical Physics)**

**February 2015**

## **ACKNOWLEDGEMENT**

First, I would like to express my gratitude and thanks to my supervisor, Dr Iskandar Shahrim bin Mustafa for supporting and helping me in the research. He brought out a lot of ideas and methods for my research. His supervision and guidance are being great help and progress in my research and theses writing.

Besides that, my greatest appreciation goes to my colleagues in Mount Miriam Cancer Hospital for helping me in the research. They offered great support and valuable knowledge in my research. They even helped me to obtain some data and measurements for the research. I would like to thank the management of Mount Miriam Cancer Hospital for letting me to conduct research in the hospital.

I would like to give thanks and gratitude to my parents. They gave me a lot of support and courage to complete the research. The moral support they gave is being great encouragement and main pillar for me to complete the research.

Lastly, I would like to thank others who had involved directly or indirectly in my research. With help and support from everyone, this research had come to a successful completion.

## TABLE OF CONTENTS

	<b>PAGE</b>
Acknowledgement	ii
Table of Contents	iii
List of Symbols and Abbreviations	v
List of Tables	vi
List of Figures	vii
Abstrak	ix
Abstract	x
<b>CHAPTER 1: INTRODUCTION</b>	
1.1 Background of the research	1
1.2 Objective of the research	2
1.3 Scope of the research	3
1.4 Outline of the research	3
<b>CHAPTER 2: LITERATURE REVIEW</b>	
2.1 Principles of wedges in radiotherapy	4
2.2 Physical wedge parameters	6
2.3 Theory of virtual wedge	8
2.4 Operation of virtual wedge	10
2.5 Studies of virtual wedge	13
2.6 Problem Statement	15
<b>CHAPTER 3: METHODOLOGY</b>	
3.1 Instrumentation and tools in the research	16
3.1.1 LINAC- SIEMENS ARTISTE	16
3.1.2 Physical wedges	17

3.1.3 Virtual wedge	17
3.1.4 I'mRT MatriXX	17
3.1.5 Solid water phantom	19
3.1.6 Farmer type ionization chamber, FC65-G	20
3.1.7 Electrometer – DOSE 1	21
3.2 Calibration of tools	
3.2.1 Calibration of LINAC	22
3.2.2 Calibration of I'mRT MatriXX	24
3.3 Data measurement	
3.3.1 Beam profiles measurement	25
3.3.2 PDD measurement	26
<b>CHAPTER 4: RESULTS AND DISCUSSION</b>	
4.1 Beam profiles for $10 \times 10 \text{ cm}^2$	27
4.2 Beam profiles for $20 \times 20 \text{ cm}^2$	33
4.3 Depth dose	37
<b>CHAPTER 5: CONCLUSION AND RECOMMENDATIONS</b>	
5.1 Conclusion	43
5.2 Recommendations	45
REFERENCES	47
APPENDICES	
Appendix A – The physical wedge dimensions	49
Appendix B – PDD of 6 MV photon commissioning data	53
Appendix C – Raw data for beam profiles measurement	54
Appendix D – Questionnaire about Availability of SIEMENS	58

## LIST OF ABBREVIATIONS AND SYMBOLS

LINAC	Linear accelerator
MV	Megavoltage, $10^6$ Volts
Z	Atomic number
PW	Physical wedge
VW	Virtual wedge
MLC	Multi leaves collimator
PDD	Percentage depth dose
SSD	Source to surface distance
MU	Monitor unit
QA	Quality assurance
QC	Quality control

## LIST OF TABLES

		<b>PAGE</b>
Table 4.1	Difference between PW and VW at distance from central axis for field size $10 \times 10 \text{ cm}^2$	30
Table 4.2	Difference between PW and VW at distance from central axis for field size $20 \times 20 \text{ cm}^2$	35
Table 4.3	Difference between PW and VW in PDD for field size $10 \times 10 \text{ cm}^2$	39
Table 4.4	PDD of all VW angle and open field for field size $10 \times 10 \text{ cm}^2$	40
Table 4.5	PDD of all PW angle and open field for field size $10 \times 10 \text{ cm}^2$	41

## LIST OF FIGURES

	<b>PAGE</b>	
Figure 2.1	Wedged isodose distribution	5
Figure 2.2	Comparison between isodose distributions of non-wedged (left) and wedged (right) for intersection of radiation beam at angle 60°	6
Figure 2.3	Side view on PW support plate (from left 15°, 30°, 45° and 60°)	7
Figure 2.4	PW (from left 15°, 30°, 45° and 60°) in MMCH, Penang	7
Figure 2.5	VW Dynamic Icon Screen Display	9
Figure 2.6	System in ready state to deliver VW	11
Figure 2.7	Opposing jaws during jaw travel	12
Figure 3.1	SIEMENS ARTISTE LINAC	16
Figure 3.2	I <sup>2</sup> mRT MatriXX	18
Figure 3.3	Graphical interface of OmniPro I <sup>2</sup> mRT	19
Figure 3.4	Farmer type Ionisation chamber, FC-65 G	20
Figure 3.5	Electrometer DOSE 1	21
Figure 3.6	Calibration setup for 6 MV photon	23
Figure 3.7	Setup for PDD measurements	26
Figure 4.1	Comparison of PW and VW angle 15° for field size 10 × 10 cm <sup>2</sup>	28
Figure 4.2	Comparison of PW and VW angle 30° for field size 10 × 10 cm <sup>2</sup>	28
Figure 4.3	Comparison of PW and VW angle 45° for field size 10 × 10 cm <sup>2</sup>	29

Figure 4.4	Comparison of PW and VW angle 60° for field size 10 × 10 cm <sup>2</sup>	29
Figure 4.5	Comparison of PW and VW angle 15° for field size 20 × 20 cm <sup>2</sup>	33
Figure 4.6	Comparison of PW and VW angle 30° for field size 20 × 20 cm <sup>2</sup>	33
Figure 4.7	Comparison of PW and VW angle 45° for field size 20 × 20 cm <sup>2</sup>	34
Figure 4.8	Comparison of PW and VW angle 60° for field size 20 × 20 cm <sup>2</sup>	34
Figure 4.9	PDD of PW and VW angle 15° for field size 10 × 10 cm <sup>2</sup>	37
Figure 4.10	PDD of PW and VW angle 30° for field size 10 × 10 cm <sup>2</sup>	37
Figure 4.11	PDD of PW and VW angle 45° for field size 10 × 10 cm <sup>2</sup>	38
Figure 4.12	PDD of PW and VW angle 60° for field size 10 × 10 cm <sup>2</sup>	38
Figure 4.13	PDD of all VW angle and open field for field size 10 × 10 cm <sup>2</sup>	40
Figure 4.14	PDD of all PW angle and open field for field size 10 × 10 cm <sup>2</sup>	41

# **PERBANDINGAN ANTARA BAJI FIZIKAL DAN BAJI MAYA UNTUK PEMECUT LINEAR**

## **ABSTRAK**

Baji biasa digunakan dalam radioterapi untuk mengubahsuai isodos dan mengurangkan intensiti radiasi melintasi saiz medan. Pemecut linear SIEMENS mengandungi dua jenis baji iaitu baji fizikal dan baji maya. Baji maya menggantikan prosedur untuk memuatkan baji fizikal apabila isodos berbaji diperlukan. Kajian untuk baji maya diperlukan agar baji maya boleh digunakan dalam aplikasi klinikal. Perbandingan profil alur dan peratus dos kedalaman untuk kedua-dua jenis baji dibuat pada empat sudut iaitu  $15^\circ$ ,  $30^\circ$ ,  $45^\circ$  dan  $60^\circ$ . Profil alur saiz  $10 \times 10 \text{ cm}^2$  dan  $20 \times 20 \text{ cm}^2$  diukur di kedalaman 5.0 cm untuk kedua-dua jenis baji. Peratus dos kedalaman saiz medan  $10 \times 10 \text{ cm}^2$  juga diukur. Baji maya mempunyai kecerunan yang hampir sama dengan baji fizikal dalam profil alur. Untuk saiz medan  $10 \times 10 \text{ cm}^2$  pada 5.0 cm hujung nipis baji, baji fizikal mempunyai dos yang lebih rendah sebanyak 3.6%, 1.6%, 2.0% dan 4.7% untuk sudut  $15^\circ$ ,  $30^\circ$ ,  $45^\circ$  dan  $60^\circ$ . Di luar saiz medan, pada 7.4 cm hujung nipis baji, baji fizikal menunjukkan dos yang lebih tinggi sebanyak 7.6%, 15.8%, 26.1% dan 25.5% untuk sudut  $15^\circ$ ,  $30^\circ$ ,  $45^\circ$  dan  $60^\circ$ . Manakala untuk saiz medan  $20 \times 20 \text{ cm}^2$ , baji fizikal juga mempunyai dos yang lebih rendah sebanyak 3.3%, 1.1%, 2.2% dan 3.9% untuk sudut  $15^\circ$ ,  $30^\circ$ ,  $45^\circ$  dan  $60^\circ$  pada 5.0 cm hujung nipis baji. Bagi perbandingan peratus dos kedalaman, baji fizikal mempunyai dos yang lebih rendah 0.5%, 0.9%, 2.0% dan 1.8% untuk sudut  $15^\circ$ ,  $30^\circ$ ,  $45^\circ$  dan  $60^\circ$  pada kedalaman 1.0 cm tetapi dos yang lebih tinggi 1.3%, 1.6%, 2.5% dan 2.2% untuk sudut  $15^\circ$ ,  $30^\circ$ ,  $45^\circ$  dan  $60^\circ$  pada kedalaman 10.0 cm. Sebagai kesimpulan, profil baji maya hampir sama dengan profil baji fizikal tetapi kurang kesan pengerasan dan kurang dos terserak di luar medan radiasi.

# COMPARISON BETWEEN PHYSICAL WEDGES AND VIRTUAL WEDGES IN LINAC

## ABSTRACT

Wedge is commonly used in radiotherapy to modify isodose distribution and reduce intensity across the radiation field. There are two types of wedge for SIEMENS linear accelerator, physical wedge and virtual wedge. Virtual wedge replaces the procedure to mount on the physical wedge when a wedged isodose is needed. The aim of this study is to facilitate the clinical application of the virtual wedge in the radiotherapy. Comparison for beam profiles and percentage depth dose of both wedges at four angles of 15°, 30°, 45° and 60° are done. Beam profiles of field size 10 x 10 cm<sup>2</sup> and 20 x 20 cm<sup>2</sup> for both type of wedges is measured at 5.0 cm depth. Percentage depth dose of both wedges for field size 10 x 10 cm<sup>2</sup> is measured. For beam profile comparison, the virtual wedge has similar profile gradient with the physical wedge. For field size 10 x 10 cm<sup>2</sup>, the physical wedge exhibits lower dose than the virtual wedge by 3.6%, 1.6%, 2.0% and 4.7% for angle 15°, 30°, 45° and 60° at 5.0 cm thin end of the wedge. Away from field size 10 x 10 cm<sup>2</sup>, at 7.4 cm thin end of the wedge, the physical wedge shows higher dose by 7.6%, 15.8%, 26.1% and 25.5% for angle 15°, 30°, 45° and 60°. Whereas for field size 20 x 20 cm<sup>2</sup>, the physical wedge shows lower dose by 3.3%, 1.1%, 2.2% and 3.9% for angle 15°, 30°, 45° and 60° at 5.0 cm thin end of the wedge. For depth dose profile comparison, the physical wedge is showing lower dose by 0.5%, 0.9%, 2.0% and 1.8% in angle 15°, 30°, 45° and 60° at 1.0 cm depth but higher dose by 1.3%, 1.6%, 2.5% and 2.2% in angle 15°, 30°, 45° and 60° at 10.0 cm depth. In conclusion, the virtual wedge profiles are almost similar with the physical wedge but less hardening effect and less scatter dose outside of radiation field.

# CHAPTER 1

## INTRODUCTION

### 1.1 Background of the research

Linear accelerator (LINAC) is a machine to accelerate particles such as electrons and protons. The particles are accelerated by an electric field created by placing a high potential difference over an insulated column. Based on Hendee *et al.* (2005), linear accelerator has been used in physics experiment since 1930s. The first linear accelerator was developed by Wideroe in 1928 to accelerate heavy ions. According to Gintzon and Nunan (1985), in 1956, Henry Kaplan utilized the linear accelerator as a tool against cancer. A two year old boy with a retinoblastoma (tumor behind an eye) is the first patient to be treated with LINAC. The boy survived with the vision intact for the rest of his life. Since then, LINAC has become essential tool to fight cancer.

Radiation beams can be modified in various ways to provide isodose curves useful for specific clinical applications in radiation therapy. Based on Evans (2006), examples of beam modifiers are lead shielding, wedge filter, and bolus. Lead shielding is used to shape the radiation beam. Multi leaves collimator (MLC) has replaced lead shielding in shaping the radiation beam. Bolus is used to increase surface dose. Bolus is usually gel or material that equivalent to water. The placement of a wedge filter in the beam produces isodose curves that intersect the central axis of the beam at some angles other than  $90^\circ$ . For high energy radiation, the wedge is constructed of high-Z material, such as lead or copper and is positioned far from the patient's skin to retain the skin-sparing advantage of high energy photons. Wedged isodose distribution is very useful for compensating irregular contour of body.

With the use of the wedge, uniformity of the dose distribution in the irregular target volume is greatly improved.

Another application of the wedge is to alter the shape of isodose curves of two beams intersect with a small hinge angle at the target volume while reducing the hotspot in the overlap beams. Conventionally, metallic wedge filter is used and placed in the beam path to obtain wedged isodose distribution.

This metallic wedge filter is called physical wedge (PW) as it needs physical object in the path of the beam to distribute the tilted isodose distribution. SIEMENS Medical Healthcare introduced Virtual Wedge (VW) in their LINAC in year 1997. VW is generated by moving one of the jaws at constant speed and at varied dose rate to deliver isodose distribution like PW. The application of VW makes treatment delivery time shorter and faster as there is no need of manual handling of wedge filter.

## **1.2 Objective of the research**

Following the potential advantages of VW in clinical practice, this research has been carried out with following objectives:

1. To compare beam profile characteristics of PW and VW for four angles 15°, 30°, 45° and 60° at field size  $10 \times 10 \text{ cm}^2$  and  $20 \times 20 \text{ cm}^2$ .
2. To compare percentage depth dose (PDD) profile of PW and VW for four angles 15°, 30°, 45° and 60° at field size  $10 \times 10 \text{ cm}^2$ .
3. To investigate the difference between PW and VW within and away of radiation field.

### **1.3 Scope of the research**

VW is a technology breakthrough in conventional radiotherapy treatment planning. VW replaces the manual procedure of mounting of PW on LINAC which subject to mechanical geometry error and time consumption for the placement of PW on LINAC. Despite VW is more beneficial for daily radiotherapy work and clinical applications, it requires more extensive quality assurance (QA) and quality control (QC) as compared to PW. Currently, PW is being used during the radiotherapy treatment in Mount Miriam Cancer Hospital (MMCH), Penang. Intense studies and researches need to be conducted for VW to be feasible in radiotherapy treatment planning. Hence, this research intends to investigate the difference between PW and VW in hope of clinical application of VW in the hospital.

### **1.4 Outline of thesis**

The thesis consists of five chapters excluding references and appendices. Chapter one is about the introduction and background of the research. Chapter two is about literature review of papers and researches that have been done on VW and the comparison of it with PW. Chapter three elaborates methodology of this research and instrumentation that is being used in throughout the research. Chapter four shows the results and data analysis of beam profiles and PDD profiles of the VW and PW. Every comparison between VW and PW is discussed in the chapter. The last chapter concluded the outcome of this research and recommendations for future investigations.

## **CHAPTER 2**

### **LITERATURE REVIEW**

This chapter is about literature review of basic principles of wedges and previous researches on PW and VW. The problem statement is mentioned in the end of the chapter.

#### **2.1 Principles of wedges in radiotherapy**

Wedges are often used in radiotherapy practice. The wedges are used to modify isodose distribution and to reduce the intensity across the beam. The wedged beam isodose curves have a tilt compared to normal beam isodose curves. The wedged profiles is shown below in Figure 2.1. Attenuation of the beam after passing through the wedge is higher at thin end of the wedge but lesser at thick end of the wedge. The difference in the attenuation of the beam across the wedge is causing the tilt in the isodose distribution. According to Khan (1994), the wedge filter changes the beam quality by attenuating the lower energy photons (beam hardening) and to a lesser extent, by Compton scattering which produces beam softening. The beam hardening effect that caused by the wedge filter alters depth dose distribution especially at larger depths.

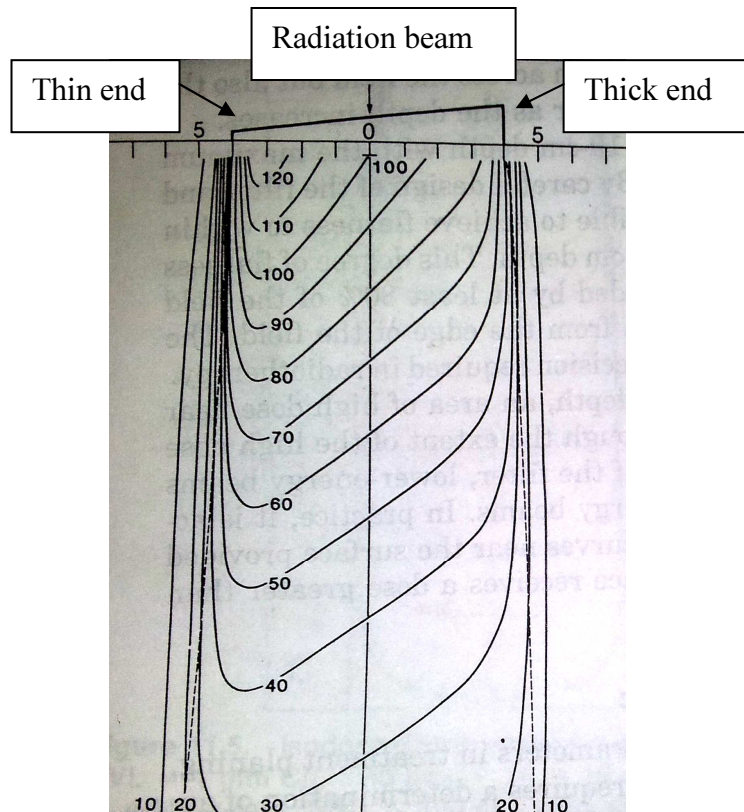


Figure 2.1: Wedged isodose distributions (Khan, 1994)

According to Hendee *et al.* (2005), for high energy radiation beam, the wedge is made of high-Z material such as lead or copper and placed far from patient's skin to keep the skin sparing effect. The wedge filter is used to decrease hotspot in intersection of two radiation beams at angles less than  $180^\circ$  apart. The comparison of isodose distribution of the intersected radiation beams at angle  $60^\circ$  apart, with and without wedge filter is shown in Figure 2.2. The highest isodose in the intersection of two beams reduced from 120% to 105% with the placement of the wedge. Besides that, the wedge improves the coverage of isodose at deeper depth of intersection from 70% to 95%.

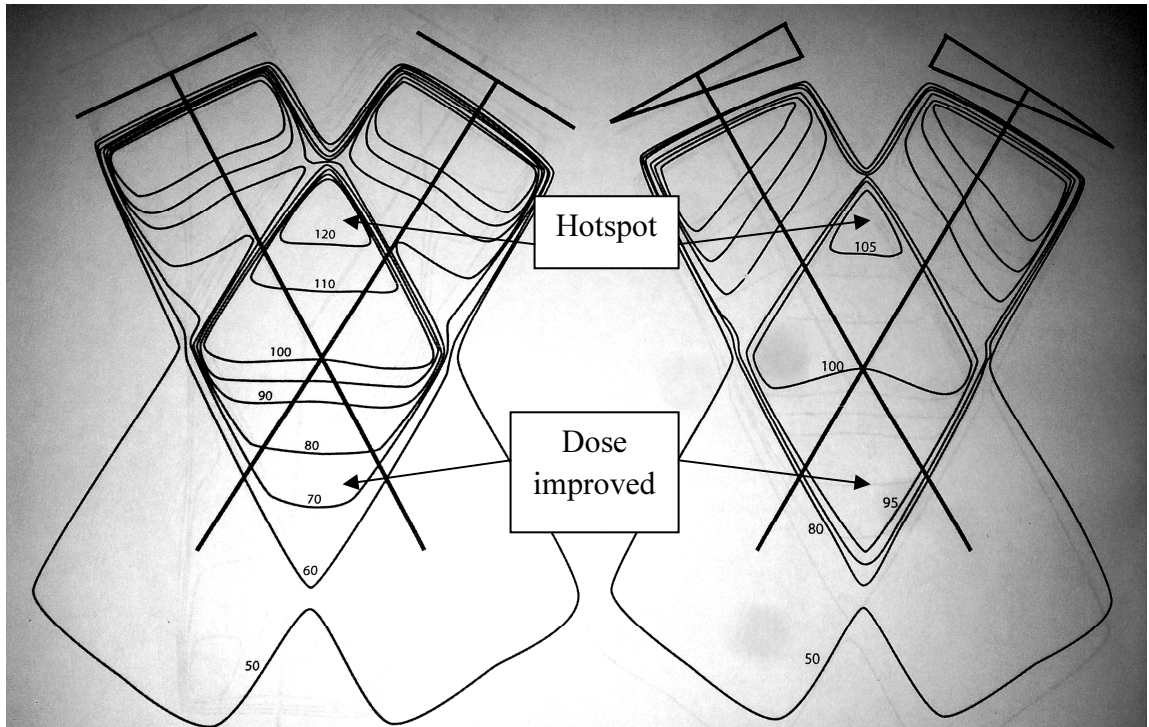


Figure 2.2: Comparison between isodose distributions of non-wedged (left) and wedged (right) for intersection of radiation beam at angle  $60^\circ$  (Hendee *et al.*, 2005)

## 2.2 Physical wedge parameters

Based on SIEMENS handbook – Physics Primer (2011), the maximum field size allowed for PW is  $25\text{ cm} \times 30\text{ cm}$  (field size in wedge direction  $\times$  non-wedge direction) for wedge angle  $15^\circ$ ,  $30^\circ$ , and  $45^\circ$ . For wedge angle  $60^\circ$ , the maximum field size allowed is  $20\text{ cm} \times 30\text{ cm}$ .

The wedge dimensions are illustrated in Appendix A, Figure A1 to A4. The width of PW for all four angles ( $15^\circ$ ,  $30^\circ$ ,  $45^\circ$  and  $60^\circ$ ) is 20.32 cm. The individual PW is mounted on support plates composed of 6.0 mm thick of aluminium. For wedge angle  $45^\circ$  and  $60^\circ$ , the plate is not part of the wedge for it is cut off to place the wedge. The side view and actual image of PW are shown in Figure 2.3 and 2.4. The wedge material is an iron alloy, EX-Cut 20 steel with physical density of  $7.81\text{ g/cm}^3$  that consists of carbon (0.23% maximum), phosphorus (0.04% maximum),

silicon (0.1% maximum), manganese (0.90% - 1.30%), sulfur (0.20% - 0.30%) and mainly iron (98.03% minimum).

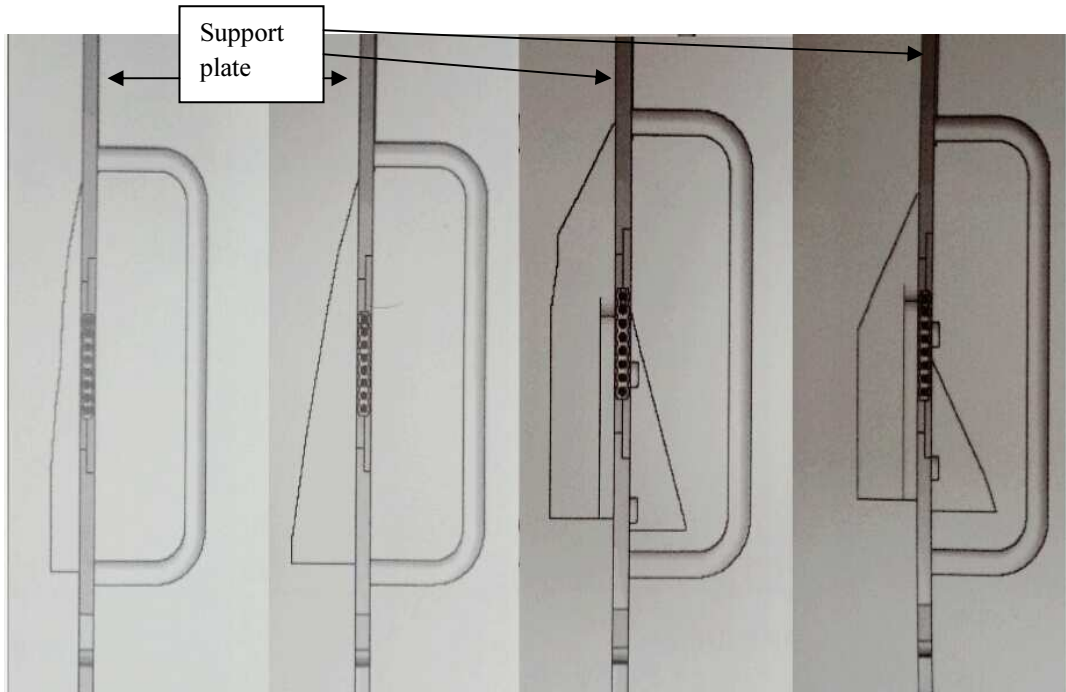


Figure 2.3: Side view on PW support plate (from left 15°, 30°, 45° and 60°)  
(SIEMENS handbook – Physics Primer, 2011)



Figure 2.4: PW (from left 15°, 30°, 45° and 60°) in MMCH, Penang

### 2.3 Theory of virtual wedge

SIEMENS Medical Healthcare set up Virtual Wedge (VW) in its linear accelerators in year 1997. The VW dose profile is formed similar to wedged isodose which previously achieved by using physical wedge (PW). Each time before use, PW needs to be mounted manually in LINAC head. The VW profile is produced by moving one of the jaws at a constant speed during beam on radiation and varying the dose rate during irradiation. Based on Rathee *et al.* (1999), the dose rate is varied according to the following equations:

$$\frac{dMU}{dt} = -TIMU \cdot K \cdot \mu \cdot \tan \theta \cdot e^{-\mu(K+S)\tan \theta}$$

and  $TIMU = MU(0)e^{\mu S \tan \theta}$

where MU(0) is the monitor unit prescribed on the central axis, S is the distance of stationary jaw from central axis,  $\mu$  is the linear attenuation coefficient of water at beam energy, K is the speed of moving jaw and  $\theta$  is the desired wedge angle. When the VW field has been programmed and accepted on LINAC console, the monitor displays a curve indicating the final positions of dynamic and stationary jaws as well as the dose to be delivered at each point across the field relative to prescribed MU on central axis. The highest monitor unit shown at the toe of the curve is TIMU.

Based on SIEMENS handbook – Physics Primer (2011), VW delivers a dose profile comparable to PW. It is achieved by controlling the movement of one of the jaws at a constant speed and varying the dose rate during irradiation.

LINAC delivers dose in monitor unit (MU) calibrated 1.0 MU per 1.0 cGy at maximum depth dose at source to surface distance, SSD = 100.0 cm. If MU is proportional with dose deliverance, the equation for number of MU at any point along VW field is:

$$MU(y) = MU_{cax} e^{-c\mu(E)y \tan \alpha}$$

$MU(y)$  = the number of monitor units to be delivered at position  $y$

$MU_{cax}$  = the number of the monitor units to be delivered at the central axis (CAX) and calculated at 10.0 cm depth

$c$  = the calibration factor

$\mu(E)$  = the mean linear attenuation coefficient for the particular energy set at the factory in  $\text{mm}^{-1}$  but need to be entered in the same units as  $y$  (usually in cm)

$y$  = the position of moving jaw at the time

$\alpha$  = the desired wedge angle at 10.0 cm depth

The Figure 2.5 is showing how VW is display in LINAC console upon delivery.

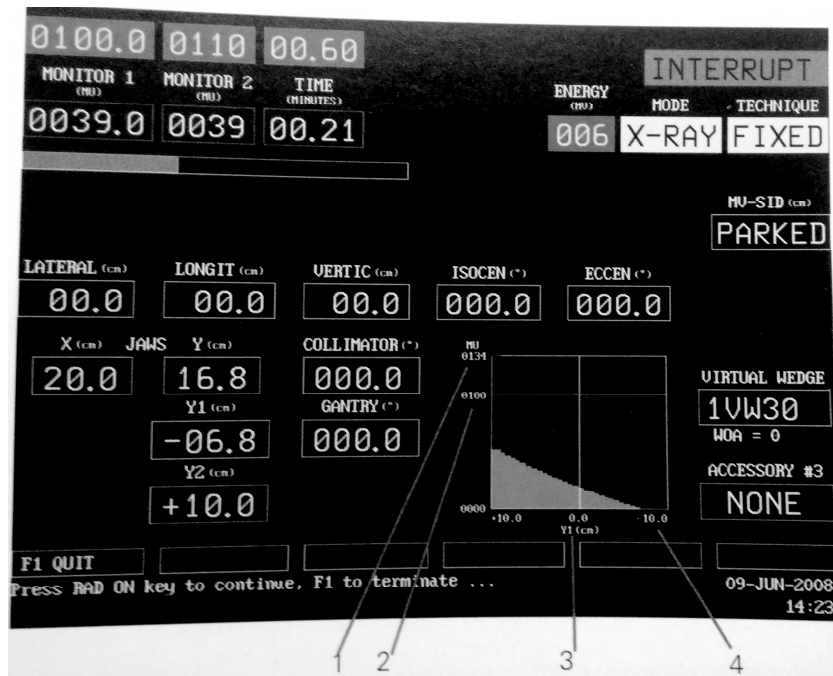


Figure 2.5: VW Dynamic Icon Screen Display. 1 =  $MU_{total}$ , 2 =  $MU_{cax}$ , 3 = moving jaw, 4 = VW Dynamic icon. (SIEMENS handbook – Physics Primer, 2011)

According to van Santvoort (1998), general equation for virtual wedge is as below.

$$MU(x) = MU(0)e^{-\mu x \tan \alpha}$$

$MU(x)$  = the number of monitor units given when a point of position  $x$  is irradiated

$MU(0)$  = the number of monitor units at  $x = 0$

$\mu$  = the linear attenuation coefficient

$\alpha$  = the wedge angle

## 2.4 Operation of Virtual Wedge

Referring to SIEMENS handbook – Physics Primer (2011), VW is delivered by constant speed of fixed jaw and changing dose rate during delivery of radiation. During delivery of VW, VW develops the correspondent of the thin end of the wedge by first irradiating a small gap between the jaws. The VW can only be achieved by using the Y jaws and not by MLC that replaces X jaws.

When VW is programmed and accepted at LINAC control console, the system moves one of the Y jaws from preset field size to starting position leaving a gap of 1.0 cm from the another Y jaw such in Figure 2.6. After that, the system carries out jaw speed test. The jaw speed test is executed by moving the jaw 0.5 cm into the 1.0 cm gap to verify the control console selected jaw speed. This speed is used by the control console to determine how the dose rate changes to deliver the preset field size and wedge angle. The jaw speed ranged from 0.02 to 2.0 cm/s.

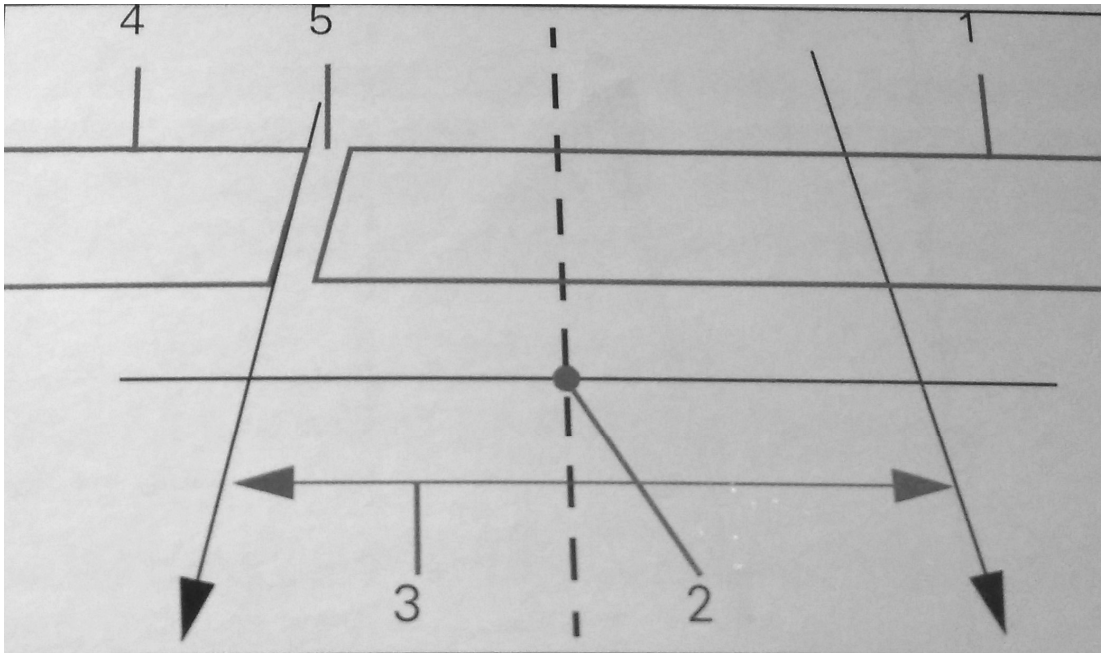


Figure 2.6: System in ready state to deliver VW. 1 = moving jaw, 2 = isocentre, 3 = preset field size, 4 = static jaw, 5 = 1.0 cm gap at starting position. (SIEMENS handbook – Physics Primer, 2011)

After the jaw speed test, the system is ready to deliver the programmed VW. The irradiation started with both jaws stationary at starting position to simulate the thin end of the wedge delivery. Then the moving jaw shifts at a constant speed to preset position of field size while the dose rate is changing. Figure 2.7 is showing the moving jaw is moving towards preset field size.

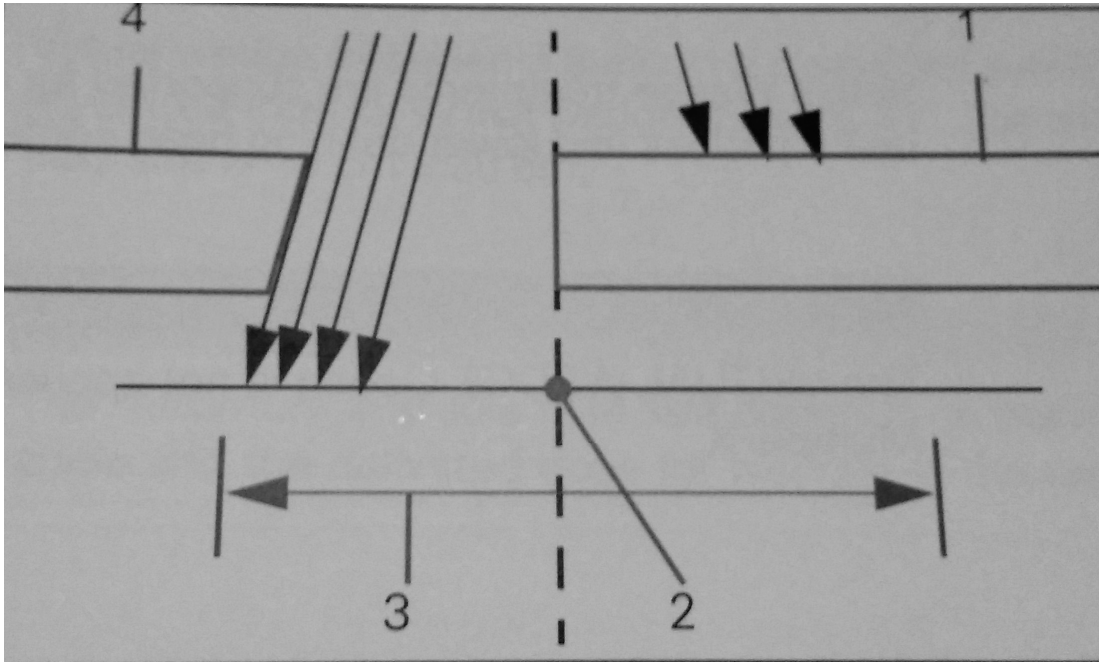


Figure 2.7: Opposing jaws during jaw travel. 1 = moving jaw, 2 = isocentre, 3 = preset field size, 4 = static jaw. (SIEMENS handbook – Physics Primer, 2011)

The amount of dose delivered from the starting position to preset field size is changing upon the programmed wedge angle. The dose rate range for 6 MV is from 40 to 300 MU/min and 10 MV is from 70 to 500 MU/min. When the preset field size is reached, the moving jaw stops and the remaining of the dose are delivered at a constant dose rate.

## 2.5 Studies of virtual wedge

Based on van Santvoort (1998), the difference of PDD between VW and open field is smaller than 0.8%. Therefore, he concluded that it is not needed to obtain PDD for large number of VW field sizes. However the PDD for PW is larger but the difference is not stated in the study. He also found out the wedge factor for VW is almost unity and the deviation from unity increases with increasing wedge angle and field size to a maximum of 3.5% for 6 MV.

According to Rathee *et al.* (1999), VW have PDD within 1% of the open beam PDD of 68% at 6 MV and 80% at 23 MV photon energies. All wedge factors for VW are equal to 1.0 within 1% except for 60° for field size 20 × 20 cm<sup>2</sup> where it deviates by 2%. The penumbra shape of the VW beam profile is identical to open field beam profile. He discussed daily and monthly quality assurance (QA) results. Daily QA for several months show deviation in ratio of two off-center chambers in wedge direction from the reference values do not exceed 1.5%. Monthly QA for beam profiles show no significant change over the time. The QA shows VW is quite stable and reproducible over the time.

Based on McGhee *et al.* (1997), VW has PDD almost same as open field PDD within 0.7%. Comparison in beam profiles between the PW and VW had been performed. The study compares both wedge at angle 60° and beam profiles at depth 5.0 cm. The highest difference in the comparison is less than 5% at thin end of the wedge. The peripheral dose in virtual wedged field is lower than the physical wedged field.

According to Zhu *et al.* (2000), PDD of PW has higher difference from PDD of the open field compare to PDD of VW. The variation in PDD between open field, PW and VW reduced as the wedge angle reduces.

For beam profile comparison, VW profiles are quite identical with PW profiles except at the thin end region of field size  $20 \times 20 \text{ cm}^2$  and  $25 \times 25 \text{ cm}^2$ . There is a considerable off-axis dose decrease in the non-wedge direction for the PW compared to the VW. PW has higher dose outside the field than VW and open field. The highest deviation between PW and VW in peripheral dose is 7% at the thin end of the wedge angle  $45^\circ$  with field size  $20 \times 20 \text{ cm}^2$  in the 6 MV beam.

Based on Attalla *et al.* (2010), they did the same comparison like Zhu *et al.* (2000). Open field has smallest PDD, followed by virtual wedged field and physical wedged field has the largest PDD. The variation in PDD between open, physical wedged and virtual wedged fields lessen as the wedge angle lessen. Physical wedged field has higher dose outside of the field than virtual wedged and open fields. The deviation in peripheral doses between VW and PW escalates from 5% to 8% at the thin end of the wedge at field size of  $10 \times 10 \text{ cm}^2$  in the 10 MV photon beam for angle  $30^\circ$  to  $60^\circ$ .

According to Chang and Gibbons (1999), there are different modalities in non-physical wedges. Among the modalities, there are enhanced dynamic wedge (EDW) by VARIAN and VW by SIEMENS for implementation of non-physical wedges in dose distribution. There are differences of EDW and VW such as method of delivery, initial and final jaw position, wedge angle selection and wedge factors. EDW delivers the dose distribution in variable dose rate and moving jaw speed but VW delivers in variable dose rate only but constant moving jaw speed. EDW initial jaw position is open and ends at 0.5 cm from fixed jaw where as VW initial jaw position is 1.0 cm from fixed jaw and ends at full open field size. EDW available angles are limited to  $10^\circ$ ,  $15^\circ$ ,  $20^\circ$ ,  $25^\circ$ ,  $30^\circ$ ,  $45^\circ$  and  $60^\circ$  while VW offers varying angles from  $15^\circ$  to  $60^\circ$  in  $1^\circ$  increment.

Both EDW and VW show less PDD compared to PW. Both EDW and VW show a little raise in PDD compared to open field due to secondary effect of exponential fluence distribution.

Lin *et al.* (2003) shared that VW permits significant time gain in practical treatment procedure as it is supported by remote procedures. VW also provides greater flexibility in practical and dosimetric setting as arbitrary wedge angles are possible for usage. When changing wedge angle for different fields within the same course of treatment, entering treatment room is no longer necessary.

## **2.6 Problem Statement**

Although conventional physical wedge (PW) is simple and easy to use but there are several limitations for conventional wedges. The thickness of lead or copper is increased linearly from the one end of the wedge to another end. Different inclination of wedge material would exhibit different wedge angle. Therefore the selection of wedge angles is limited by the amount of PW. Due to the physical mounting of wedge filter on LINAC, the design of the PW requires a holder for it to slot in the accessory holder on the LINAC. Hence, the usable field size with PW is smaller than the maximum field size available in the LINAC. During application of PW, radiotherapist is required to entering the treatment room to mount PW on LINAC. This manual procedure consumes more time thus increases the overall treatment delivery time to the patient.

In Malaysia, there are about 26 radiotherapy centres including private and government sectors. Out of 26 centres, half of the centres is using SIEMENS LINAC but only one centres using VW. The sample of questionnaire is shown in Appendix D.

## **CHAPTER 3**

### **METHODOLOGY**

This chapter is about method and procedure that performed in this research. Section 3.1 is about instrumentation and tools used in the research. Section 3.2 is about calibration of tools and data measurement.

#### **3.1 Instrumentation and tools in the research**

Subchapter 3.1.1 to 3.1.7 is about instrumentation and tools that used for the research.

##### **3.1.1 LINAC – SIEMENS ARTISTE**

SIEMENS ARTISTE LINAC is installed and commissioning in Mount Miriam Cancer Hospital, Penang on 2005. It is equipped with X-ray photons 6 MV and 10 MV, electron energies of 6 MeV, 9 MeV, 12 MeV, 15 MeV, 18 MeV, and 21 MeV. It is also equipped with 160 MLC with 0.5 cm thick leaves. The LINAC is shown in Figure 3.1.

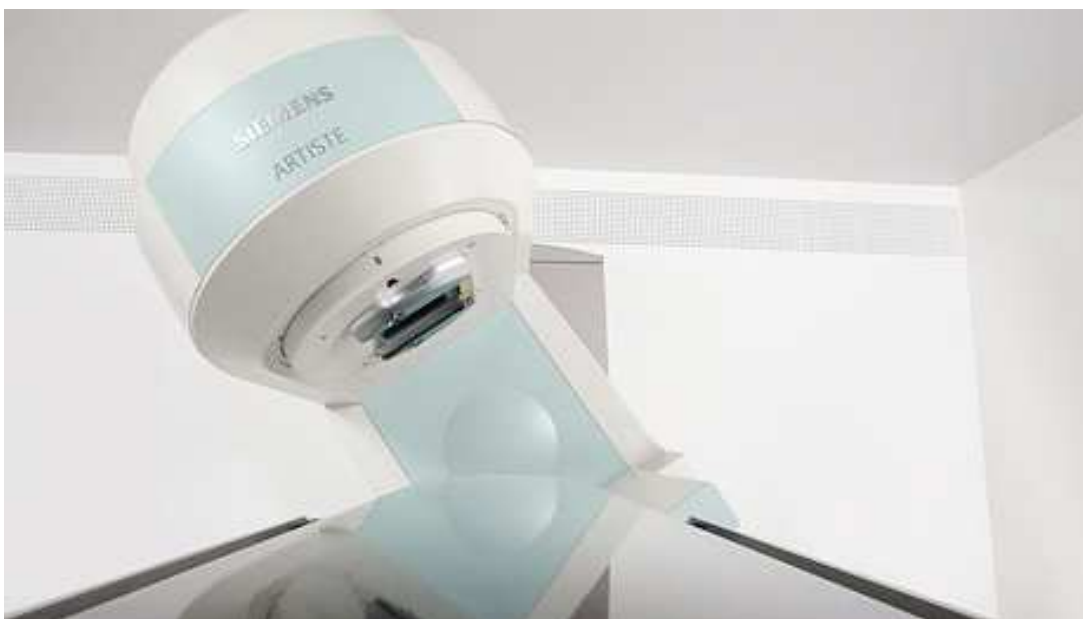


Figure 3.1: SIEMENS ARTISTE LINAC (Courtesy to SIEMENS)

### **3.1.2 Physical Wedges**

PW are varying in fixed angle of 15°, 30°, 45° and 60°. Each individual PW is mounted on support plate of 0.6 cm thick aluminum. The wedge material is composed of an iron alloy, EX-CUT 20 steel with a physical density of 7.81 g/cm<sup>3</sup>. The details of material composition are mentioned in the chapter 2. Maximum field size for all physical wedges except wedge 60° is 30 cm × 25 cm while wedge 60 degrees is 30 cm × 20 cm. The wedges are shown in Figure 2.4.

### **3.1.3 Virtual Wedge**

VW is generated by moving a collimating jaw at constant speed while varying dose rate within the limits of 10 – 300 MU/min. Any of the four jaws can be used to generate VW. In practice, only Y jaws can be used because the X jaws are replaced by MLC. The details of VW are mentioned in chapter 2.

### **3.1.4 I'mRT MatriXX**

I'mRT MatriXX (refer to Figure 3.2) is a 2-dimensional array consists of 1020 ion chambers arranged in 32 × 32 grids. The maximum field size for measurement at SSD = 100 cm is 24.4 × 24.4 cm<sup>2</sup>. Distance between the chambers is 0.762 cm. The detector type is vented parallel plate ion chamber. When irradiated, the air in the chamber is ionized. The released charge is separated by means of electrical field between the bottom and the top of electrodes. The current, which is proportional to the dose rate, is measured and digitalized by a non-multiplexed 1020 channels current sensitive analog to digital converter. The measured data are transmitted to a PC via a standard Ethernet interface.

The software integrated with the I'mRT MatriXX is OmniPro I'mRT version 1.5. The software interface is shown in Figure 3.3. There is an absorber material on top of the I'mRT MatriXX with density  $1.06 \text{ g/cm}^3$ . The thickness of the material is 3.3 mm.



Figure 3.2: I'mRT MatriXX (Courtesy to IBA Dosimetry)

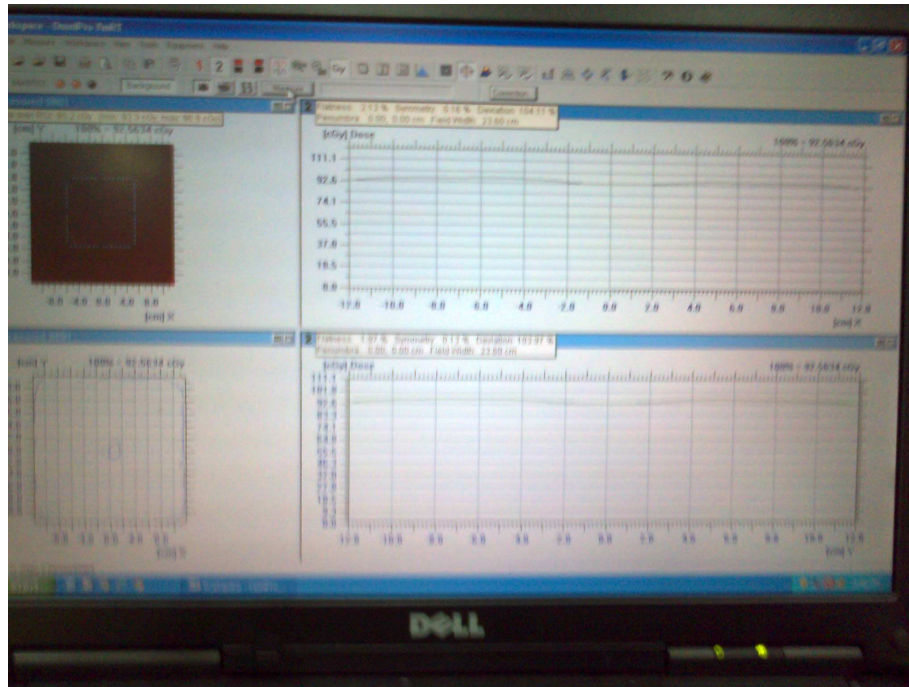


Figure 3.3: Graphical interface of OmniPro I'mRT

### 3.1.5 Solid Water Phantom

Solid water phantom is water equivalent material to represent the human tissue. The solid water phantom is from Gammex RMI, Middleton, WI. The density of the solid water phantom is  $1.04 \text{ g/cm}^3$ .

### 3.1.6 Farmer type ionization chamber, FC65-G

Farmer type chamber, FC 65-G is an air ionization chamber with graphite wall (refer to Figure 3.4). The active nominal volume of the chamber is  $0.65 \text{ cm}^3$ . The total active length of the chamber is 23.1 mm. It is used for absolute dosimetry in radiation therapy and used as standard reference detector for reference dosimetry and scientific applications.



Figure 3.4: Farmer type Ionization chamber, FC65-G

### 3.1.7 Electrometer – DOSE 1

Electrometer that used in the research is Scanditronix Wellhofer Dosimeter, DOSE 1 (refer to Figure 3.5). DOSE 1 is a single channel electrometer for measurement of absorbed dose. DOSE 1 can set up bias voltage up to  $\pm 500$  V and measuring from 40 pC to 1.0 C at 0.1 pC resolution.



Figure 3.5: Electrometer DOSE 1

## 3.2 Calibration of tools

Subchapter 3.2.1 to 3.2.2 is about calibration of LINAC and I'mRT MatriXX before taking data measurement of beam profiles and PDD profiles.

### 3.2.1 Calibration of LINAC

The LINAC is calibrated routinely by using solid water phantom fitted with Farmer type ionization chamber, FC65-G and electrometer, Dose 1. The ionization chamber and electrometer is shown in Figure 3.4 and Figure 3.5. For 6 MV photon calibration setup, 5.0 cm solid water phantom slab is built up on top of ionization chamber and 10.0 cm solid water phantom slab is placed below the ionization chamber to counter backscattering effect. The field size for calibration is  $10 \times 10 \text{ cm}^2$ . The SSD is set at 100.0 cm. The setup is shown in Figure 3.6. The Farmer type ionization chamber is then connected to electrometer, Dose 1 with extension connector and placed into customized solid water phantom slab. 100 MU of 6 MV photon beam is delivered and charge value is obtained from electrometer. This procedure was repeated for five times to obtain the average of the measured charge. The measured dose is the product of average of the measured charge (M), correction factor of temperature and pressure ( $C_{TP}$ ) and product of all factors for the chamber and beam energy ( $N_D \times P_U \times P_S \times S_{w,air}$ ). The equation is shown as below and based on IAEA TRS 277 (1997).

$$\text{Dose at } d_{\max} = (M \times C_{TP}) \times (N_D \times P_U \times P_S \times S_{w,air})$$

The product of all factors is product of absorbed dose to water calibration coefficient ( $N_D$ ), perturbation correction ( $P_U$ ), recombination correction ( $P_S$ ) and stopping power ratios water and air ( $S_{w,air}$ ).

The measured dose is then compared with commissioning data of 6 MV PDD in 5.0 cm equivalent depth of water. The PDD of 6 MV photon is shown in Appendix B figure B1. At 5.0 cm depth and  $10 \times 10 \text{ cm}^2$  field size, the PDD value for 6 MV is 86.5%. The tolerance of the calibration is 2%. If it is out of tolerance, then the LINAC output will be tuned in LINAC service mode.

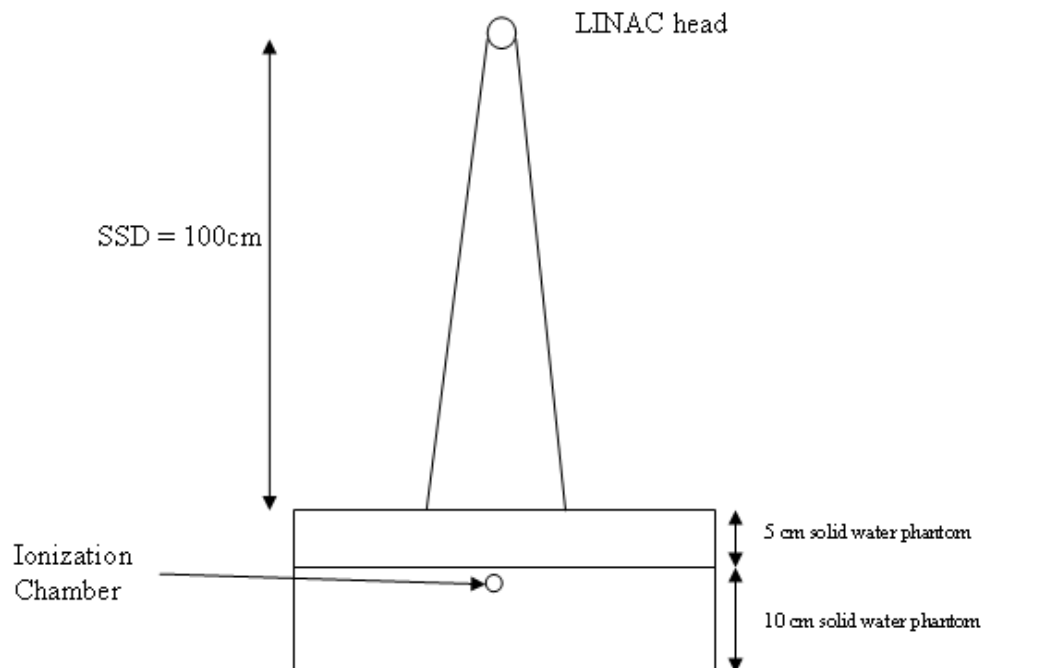


Figure 3.6: Calibration setup for 6 MV photon

The calibration is done for low dose rate, 30 MU/min and high dose rate 300 MU/min for 6 MV photon.

### **3.2.2 Calibration of I'mRT MatriXX**

The I'mRT MatriXX is cross-calibrated in the same way as LINAC calibration. From the commissioning data of the LINAC, PDD of 6 MV at 5.0 cm depth is 86.5%. PDD of 6 MV is shown in Appendix chapter figure B1. So the I'mRT MatriXX is set up and calibrated in the known PDD value. 4.7 cm thick of solid water phantom is placed on the I'mRT MatriXX as there is absorber material 0.3 cm thick. 100 MU of 6 MV is delivered and the I'mRT MatriXX obtained intensity signal for  $10 \times 10 \text{ cm}^2$  field size at central axis total of four ion chambers. The absolute dose calibration factor was obtained by averaging the four ion chamber measurements and applied to whole array of ion chambers for absolute dose measurement.